3.0 Field Trial Results

3.1 Hydrology

Rainfall-runoff data from the cap site, for the three storm events occurring on 261296, 010197, and 230197 were used to calibrate the DISTFW model using the non-linear regression package NLFIT. The parameters Cr and ϕ, S_ϕ and ϕ, and Cr and e_m were fitted firstly, with Sorptivity found to be effectively zero for all calibration runs, and was set to be zero for subsequent investigations. Hydrographs, and cumulative rainfall for each of these 3 significant events are presented in Figure 3.1.1.

The parameters were calibrated using individual storm events, whilst the next stage incorporated calibration of multiple storm events (using all three of these storms together). The purpose of multiple regression analysis was to characterise an average hydrologic behaviour for the cap site, and consequently the gully catchment.

The data appears well fitted with error in the estimation of Cr ranging between 17 and 27%, whilst em ranged between 3.8 to 4.9%, and ϕ between 5.6 and 15% appear to be within acceptable ranges.

Prospective errors in estimation of Cr, em and ϕ are: 15.2%, 3.5%, and 6.8% respectively, suggesting additional two storm events provide marginal improvement in estimating parameter values.

Table 3.1.1: Calibration results for cap site for individually fitted storm events: 261296, 010197, and 230197. Calibrated value and standard deviation is expressed.

Event	Cr (mm/hr$^{0.5}$)	e_m	ϕ (mm/hr)
261296	25.59 ± 6.92	2.52 ± 0.12	7.27 ± 1.05
010197	5.61 ± 0.95	1.55 ± 0.06	16.34 ± 0.92
230197	5.44 ± 0.70	1.27 ± 0.05	6.57 ± 0.99

Table 3.1.2: Joint calibration results for the cap site for the three designated storm events (mean ± s.d.).

Event	Cr (mm/hr$^{0.5}$)	e_m	ϕ (mm/hr)
average	7.90 ± 1.20	1.72 ± 0.06	11.74 ± 0.80

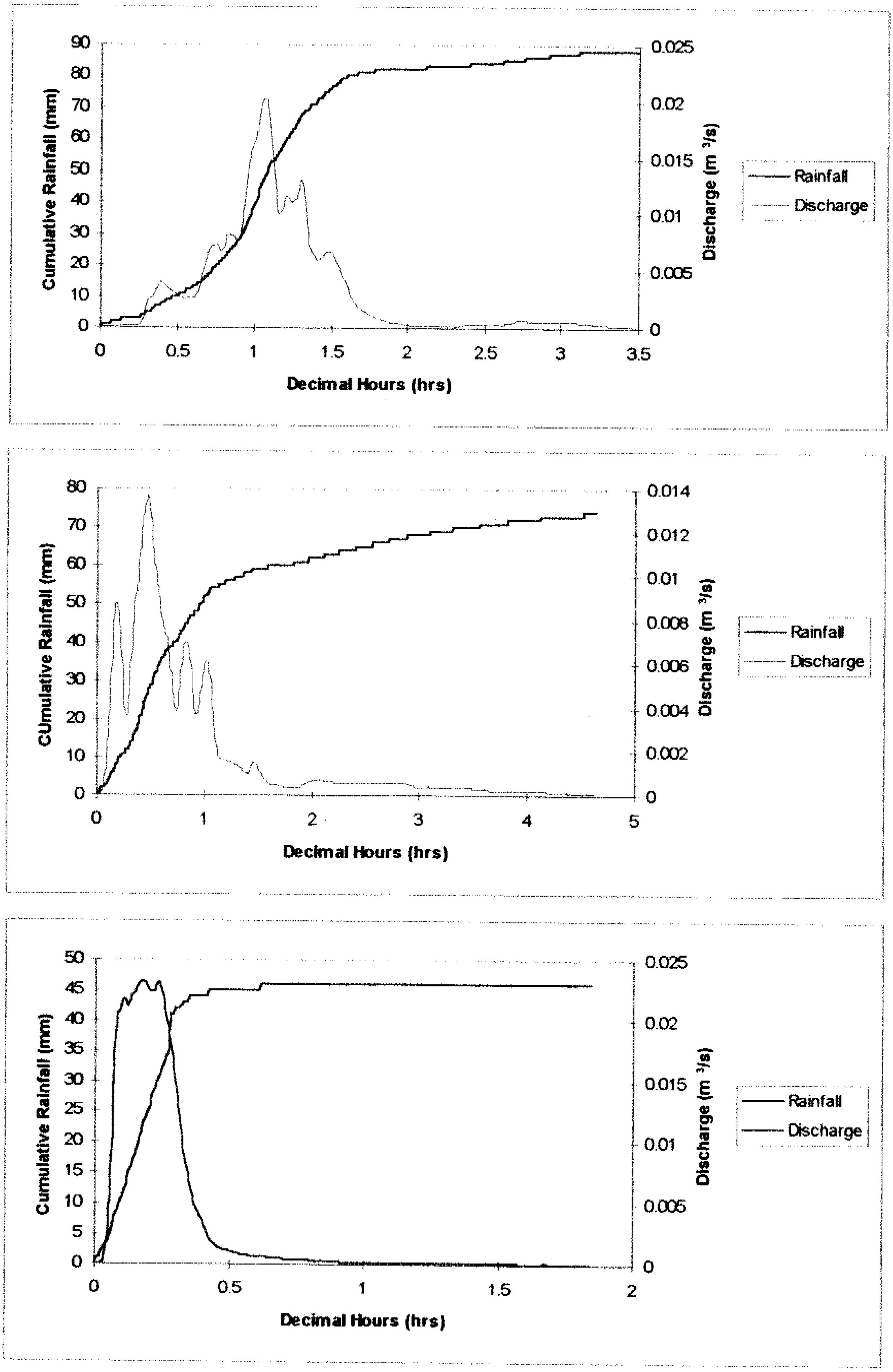

Figure 3.1.1: Observed runoff hydrographs and cumulative rainfall plots for cap site storm events monitored on: a) 261296, b) 010197, and c) 230197.

Table 3.1.3: Calibration results for gully catchment using individual storm events (mean ± s.d.).

Event	Cr (mm/hr$^{0.5}$)	e_m	ϕ (mm/hr)
261296	35.29 ± 3.33	2.67 ± 0.12	6.59 ± 1.09
010197	67.45 ± 7.15	1.78 ± 0.08	29.64 ± 1.00
230197	82.42 ± 5.19	1.36 ± 0.06	5.18 ± 1.18

Table 3.1.4: Calibration results for the catchment, for runoff events fitted simultaneously (mean ± s.d.).

Event	Cr (mm/hr$^{0.5}$)	e_m	ϕ (mm/hr)
average	85.87 ± 6.55	1.84 ± 0.06	24.74 ± 0.79

The next stage of the rainfall-runoff calibration involved approximating the discharge from the gully catchment itself. As outlined above, an approximate scaling was employed, as installation of monitoring equipment at the head of the gully network would have disturbed water flow. Adjustments were made to the catchment description file *.fw, and a multiplier factor of 12.204 was used for each of the runoff (*.ro) files. The model parameters Cr, em and ϕ were fitted once again, with Sorptivity S_ϕ again found to be effectively zero. From Table 3.1.3, the error in estimate of Cr, em and ϕ were (6.3% to 10.6%), (4.4% to 5.5%), and (3% to 22.8%) respectively. These values compare well with Table 3.1.1, noting that error bounds are only exceeded for ϕ, with event 230197. Errors in estimation of Cr, em and ϕ are 7.6%, 3.3%, and 3.2% compare favourably with results from Table 3.1.2. Assumptions regarding the effect of scaling up of discharge-runoff data from cap site to be representative of gully catchment seems to have been a reasonable one. The hydrographs and corresponding predictions for gully catchment are illustrated in Figure 3.1.2 below, with these events adopted for calibration of storm events into the SIBERIA landform model, representative if the catchment batter study site.

Further investigation and comparison may be made with results from previous hydrology studies conducted on the cap site, Evans in prep., however these considerations are beyond the focus of this study. It is noted from Table 3.1.1, the variation between values of ϕ, and em are replicated in fitting for cap site against the gully catchment. However conveyance (flow geometry, Cr) for the first event seems to remain small, characteristic of the nature of the storm event observed in Figure 3.1.1a. An estimate for e_m of 1.72, and 1.84 for cap site and gully catchment, is consistent with theoretical interpretation of surface roughness of the two sites.

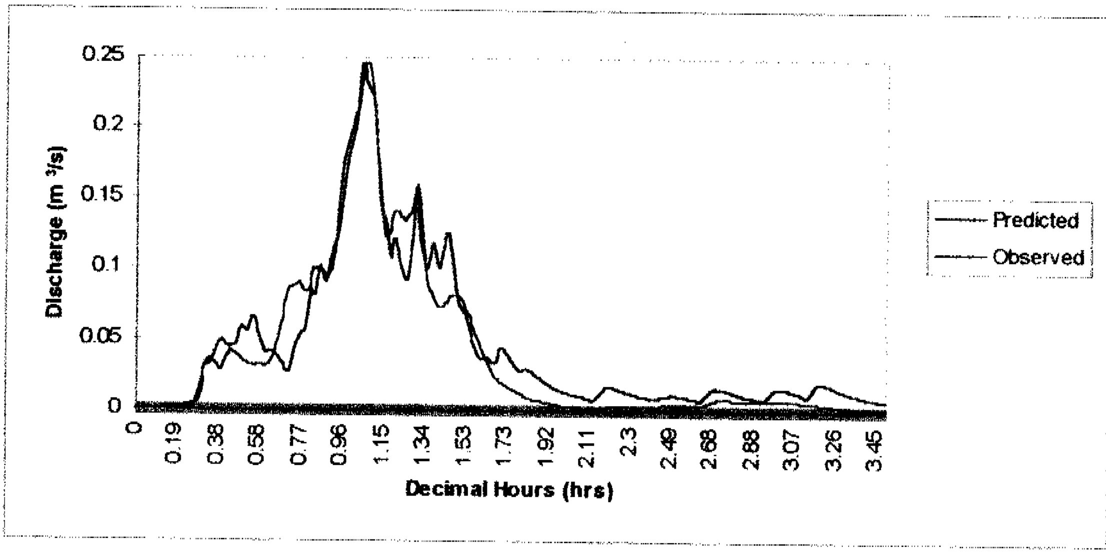

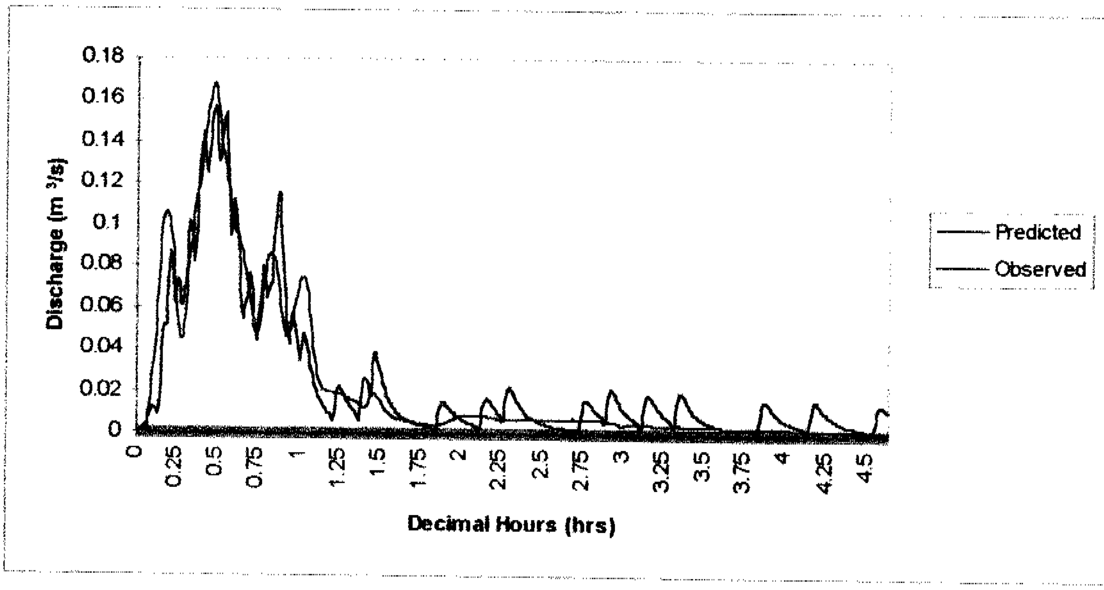

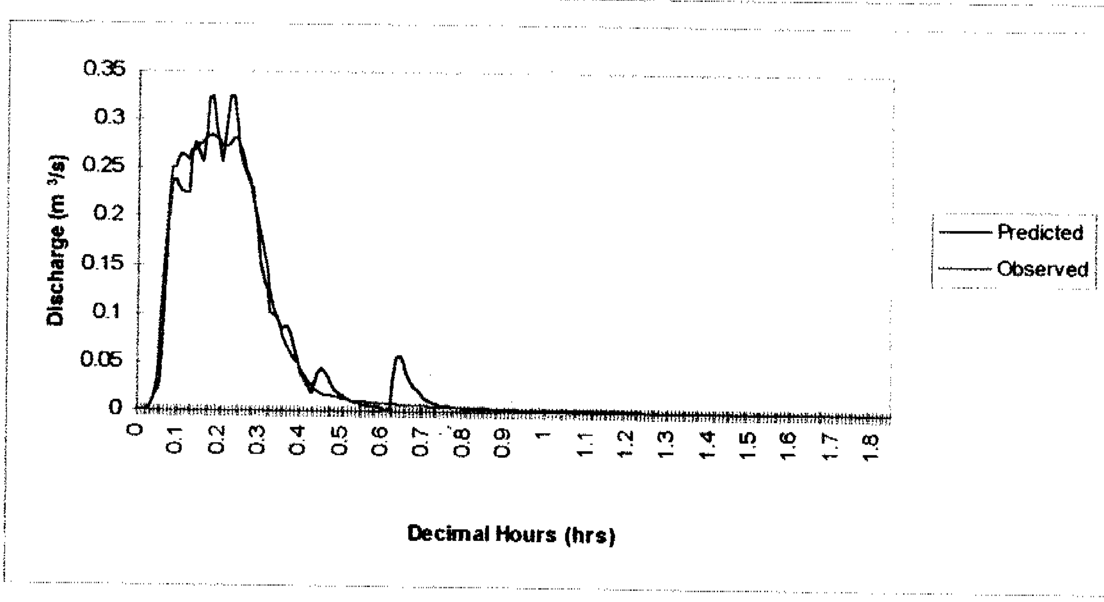

Figure 3.1.2: Gully Catchment hydrographs and predictions from the multiple regression fitting of all three significant storm events; a) 261296, b) 010197, and c) 230197.

3.2 Gully Development

Formation of a gully on the steep batter slopes of the NWRD was monitored during the 96-97 Wet Season. Analysis of the characteristic and nature of the initiation and development of the gully provides a field basis for continuing validation of the SIBERIA model.

The original topography of the site is described in detail above, with an inherent large degree of complexity in both form and constituency. The spatial variability in the waste rock material, illustrated in Figure 2.7 was significant, with the site being exposed and undisturbed for the past several years. Geochemical weathering processes which by their nature, are extremely significant in the region, were considered dominant factors in formation of the soil type material found on the upper surfaces of the slope. The fine particle material on the upper slopes was expected to erode quickly, exposing the coarser grade material below. The upper section of the slope Rows A to C had a very thin layer of fine material compared to between Rows E to F to G, where accumulation of 40cm of fine mulch had occurred. This may have been a product of the construction process of the rock dump, or dependent on the nature of weathering that has occurred.

The erodibility of the waste rock material was expected to be highly differential, with spatial heterogeneity having dramatic consequences on the final shape and form of the instigated gully network. The site characteristics were segregated into the following categories: heterogeneity, differential erodibility with depth and impact of inlet width at the top of the batter slope. The impact of these site characteristics will be the subject of these investigations, with incorporation of these factors into consequent prediction efforts.

The geometry of the batter site is complex with concavo-convex slope. A change in curvature occurs between Row H - Row I, as illustrated in Figure 2.6. Results from field trial observations with excavation on the upper sections and deposition onto lower sections followed expected theoretical behaviour mechanisms. Initial profiles of the batter site also suggested that incision of the top slopes of the highwall would occur. The degree of erosion at this transition point between the gully catchment and the batter slope was influenced by the relatively thin layer of fine material in this region, and the larger reservoir inadvertently created behind the leading bund wall. This reservoir effectively raised the entry notch about 30cm before runoff from the catchment could enter the gully, with only relatively intense storm events of significant magnitude generating enough runoff for erosion to occur.

Figure 1.3.2 above outlines the nature of the equilibrium slope formation, far removed from the initial study site characteristics. However the physical attributes of the site are dictated, and hence the location of batter slopes, by the character of the final design solution.

During the monitoring period there were numerous storm events, with many averaging 20 to 30 mm in total. Other studies conducted during the Wet Season, (Bell, 1997) examine these numerous storm events in greater detail.

Three storm events were considered to be significantly large, instigating and directly altering the dimension, depth and length of the gully once formed. As described in Section 3.1 above, these events totalled 89mm, 79mm and 45mm respectively and occurred on 261296, 010197, and 230197 respectively.

The inlet and outlet points of the gully were significant with discharge runoff entering the gully from the 7200 m^2 catchment area above, and exiting the gully site via a flume located at the base of the slope. Measurements of suspended sediment concentration were taken at the base of the batter slope from the large flume remaining from previous erosion studies, although these samples proved inconsequential to this study. Hydrological data from the cap site, was monitored electronically with average discharge entering the gully estimated and incorporated in calibration of the landform model.

Two measurement techniques were used to ascertain the amount of material shifted proceeding each significant storm event. The intensive monitoring of cross-sectional areas at each of the 10 designated transects was used to generate an approximate picture of the gully form.

An extensive survey regime of the site during the middle of the Wet Season, and a complimentary survey of the site before and after the completion of the monitoring period was used to support findings from the cross-sectional area analysis. From the measurement techniques used on the site, the characteristic of gully formation, with areas of deposition and erosion, was determined.

Inherent difficulty in interpretation of results from this study included erosional development between monitoring rows, and smothering of erosion pins on the lower sections. Problems associated with the use of the erosion pins are highlighted above, with results devised from these dependent on the survey work conducted before the commencement of monitoring period and were not considered of high importance.

Other aspects of the field trial that were not incorporated included the assessment of mean particle diameter as a function of depth as the gully evolved. Estimates of the depth-erodibility relationship coefficients were conservative based on these incomplete estimations from Figure 4.3.7 and alike.

Table 3.2.1 below, summarises the findings from this intensive study, with estimates of the amount of material mobilised from each storm event determined from difference between surface profiles for each of the 3 storm events. Maximum erosion depths and overall profile development are however considered the most important findings in this study. The width of the gully and distance between rows is presented in Table 3.2.2 below, with little development in the upper sections once the gully was initiated. The following figures also attempt to highlight the characteristic of the evolution of the batter slope profile to its' present form.

Figure 3.2.1, 3.2.2, and 3.2.3 illustrate the results of the survey study conducted before the commencement of the Wet Season, during the Wet Season (January 16th) and after the cessation of monitoring period (April 97).

Figures 3.2.4, 3.2.5 and 3.2.6 were derived from the cross-sectional analysis. These surfaces were then used in comparison to original topography, and each consequent event, with the difference between consecutive events indicating regions of deposition

Surface Topography: Pre-Wet Season

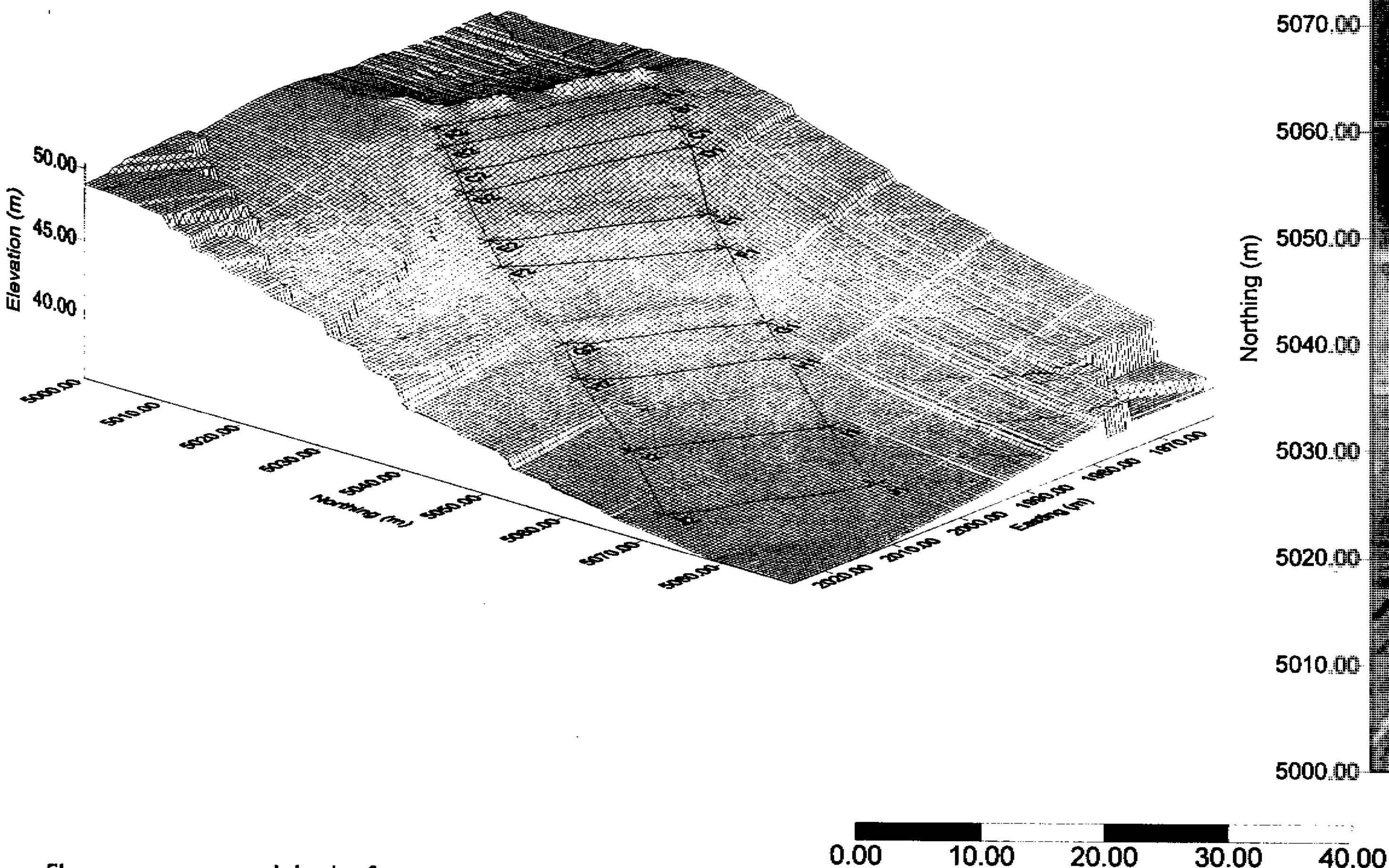

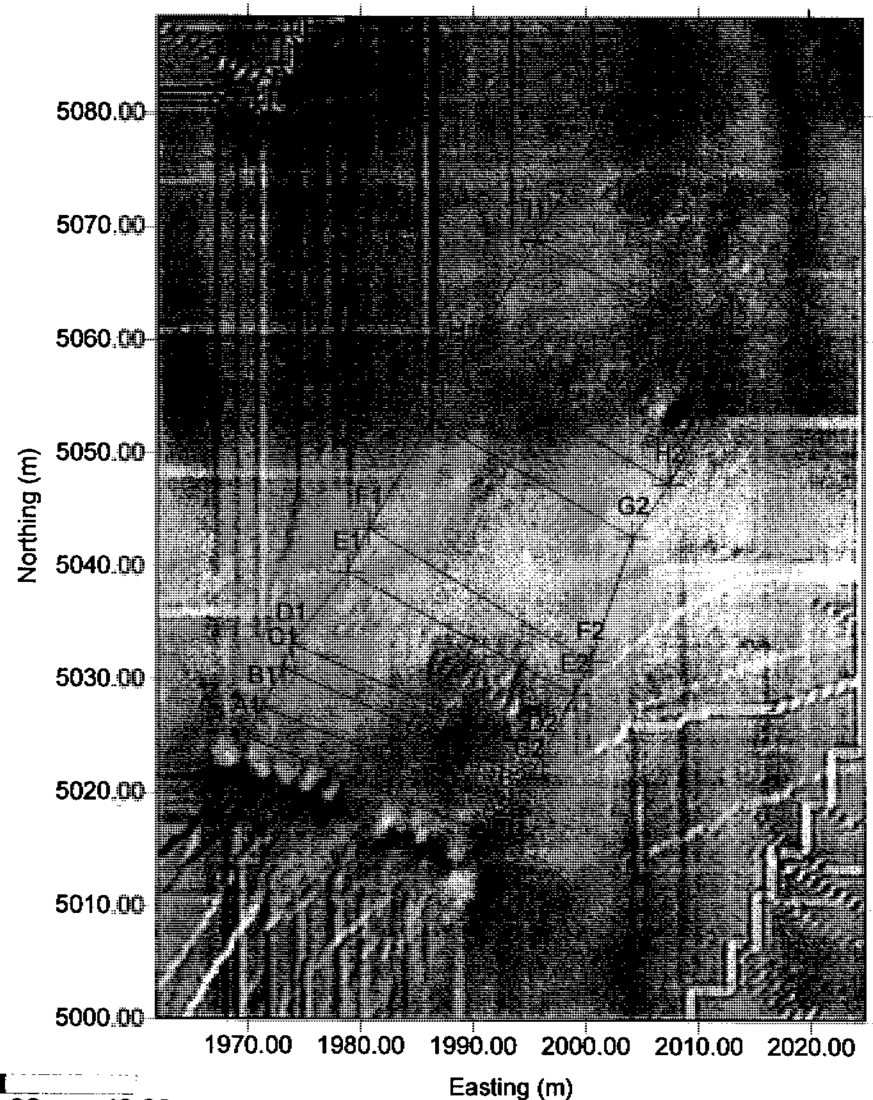

filename: survey-original.srf

Figure 3.2.1: Three surveys were conducted during the field trial phase of this investigation. The first survey represents the batter slope before the commencement of gulling and was conducted before the start of the Wet Season.

Surface Topography: Mid-Wet Season

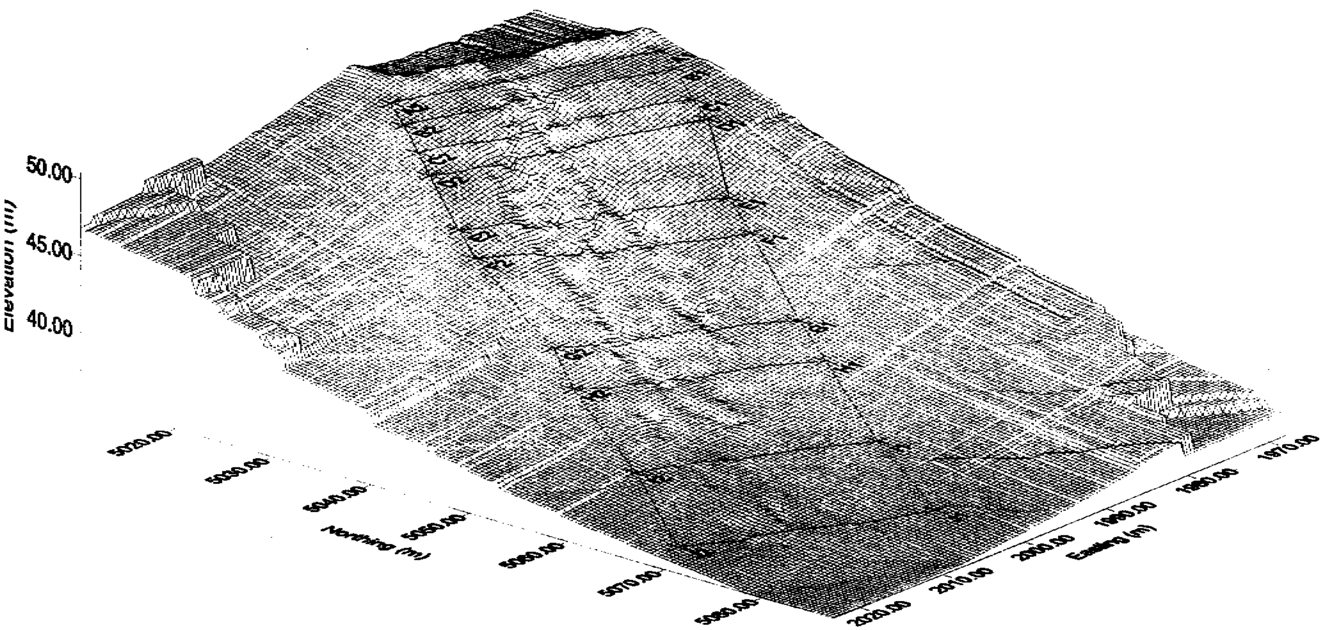

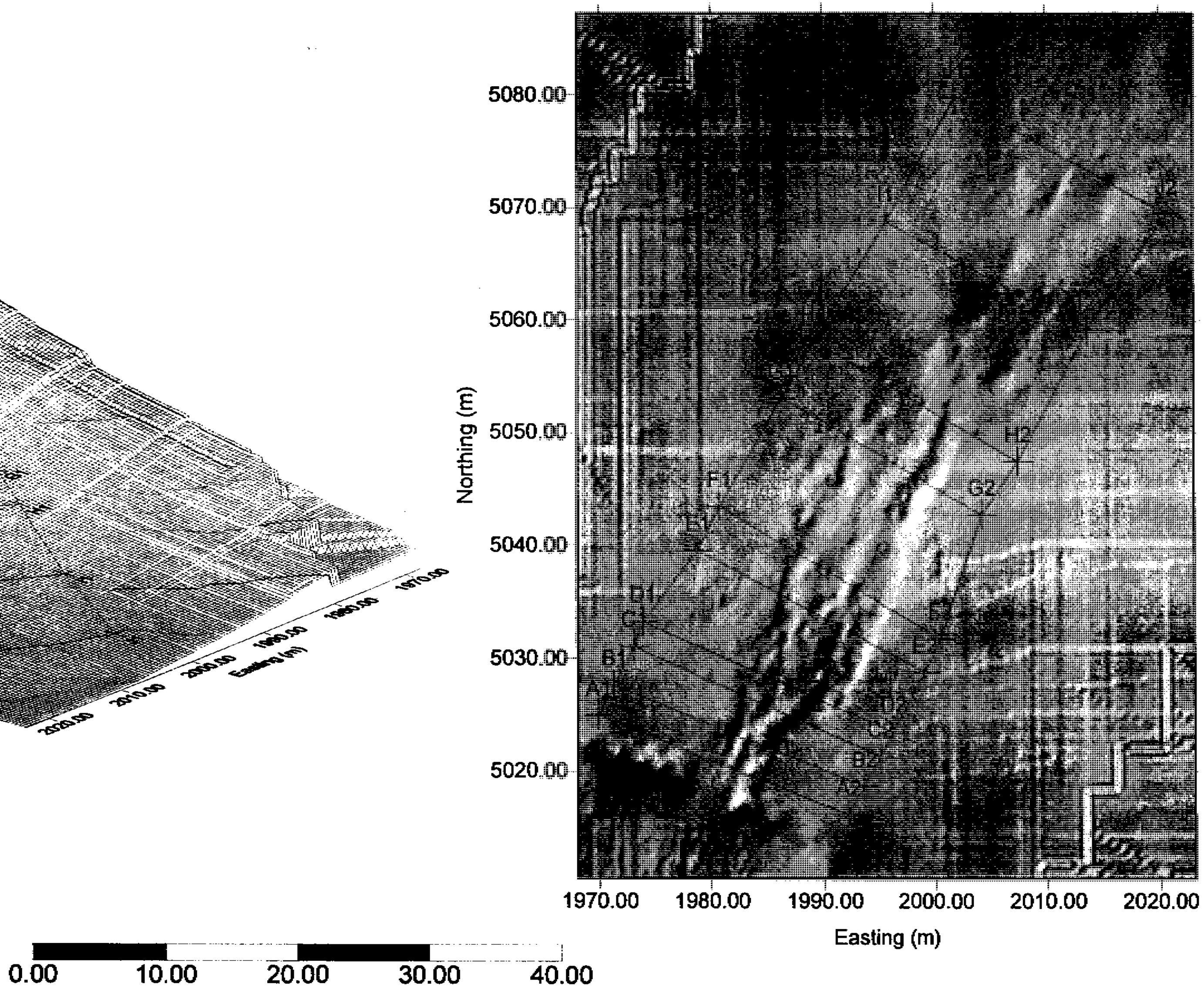

filename: survey-midwet.srf

Figure 3.2.2: The next survey was conducted mid-way through the monitoring period on 16th January, where the first two storm events are compared to this landscape.

Surface Topography: Dry Season

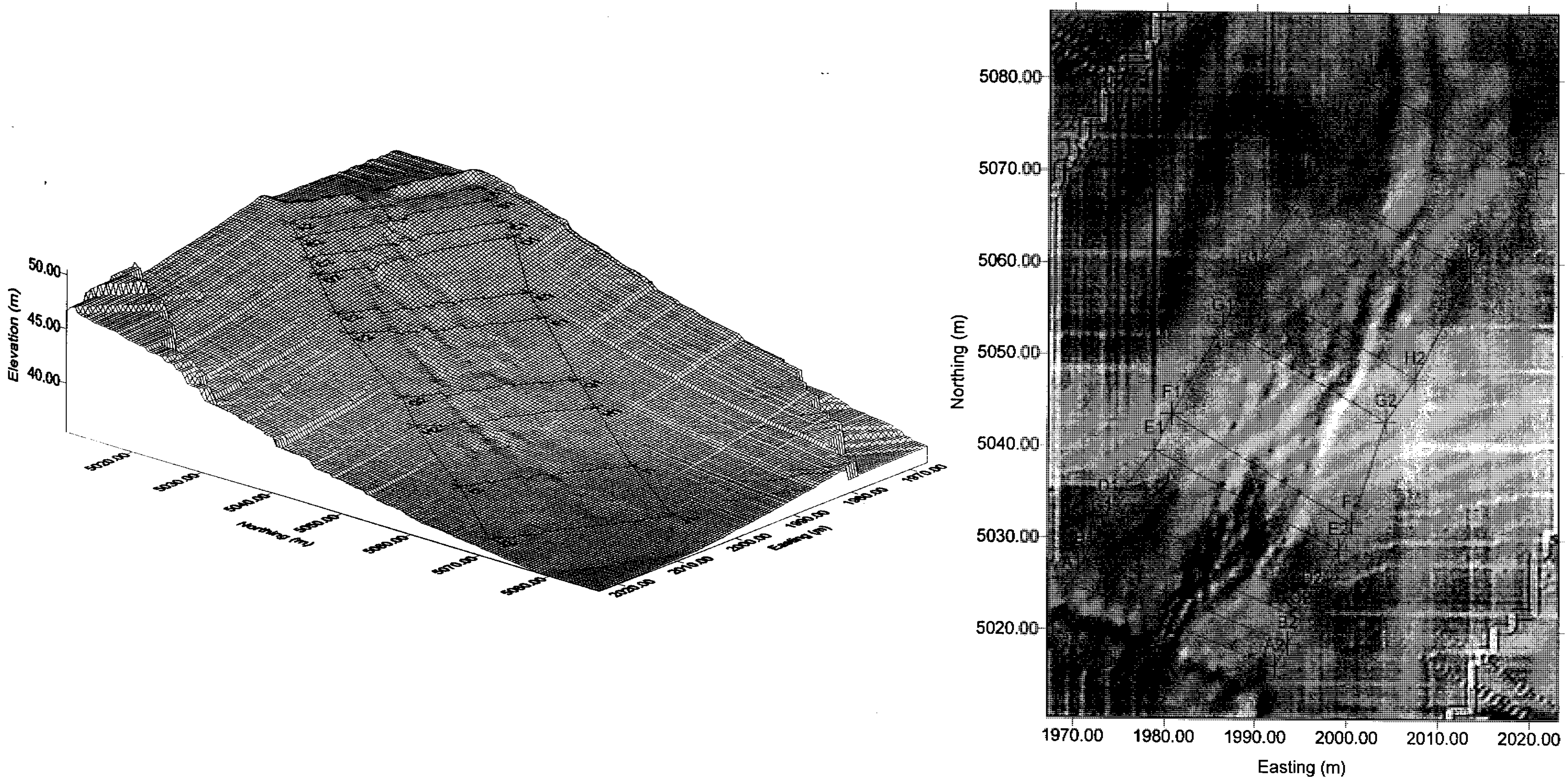

filename: survey-dry.srf

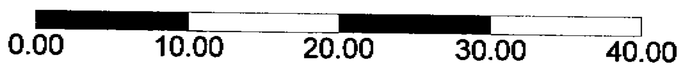

Figure 3.2.3: The final survey was conducted after the cessation of monitoring at the end of the Wet Season, although the detail of this survey was less than that seen in Figure 3.2.2, the continuing development of the gully can be observed to the bottom of the batter slope.

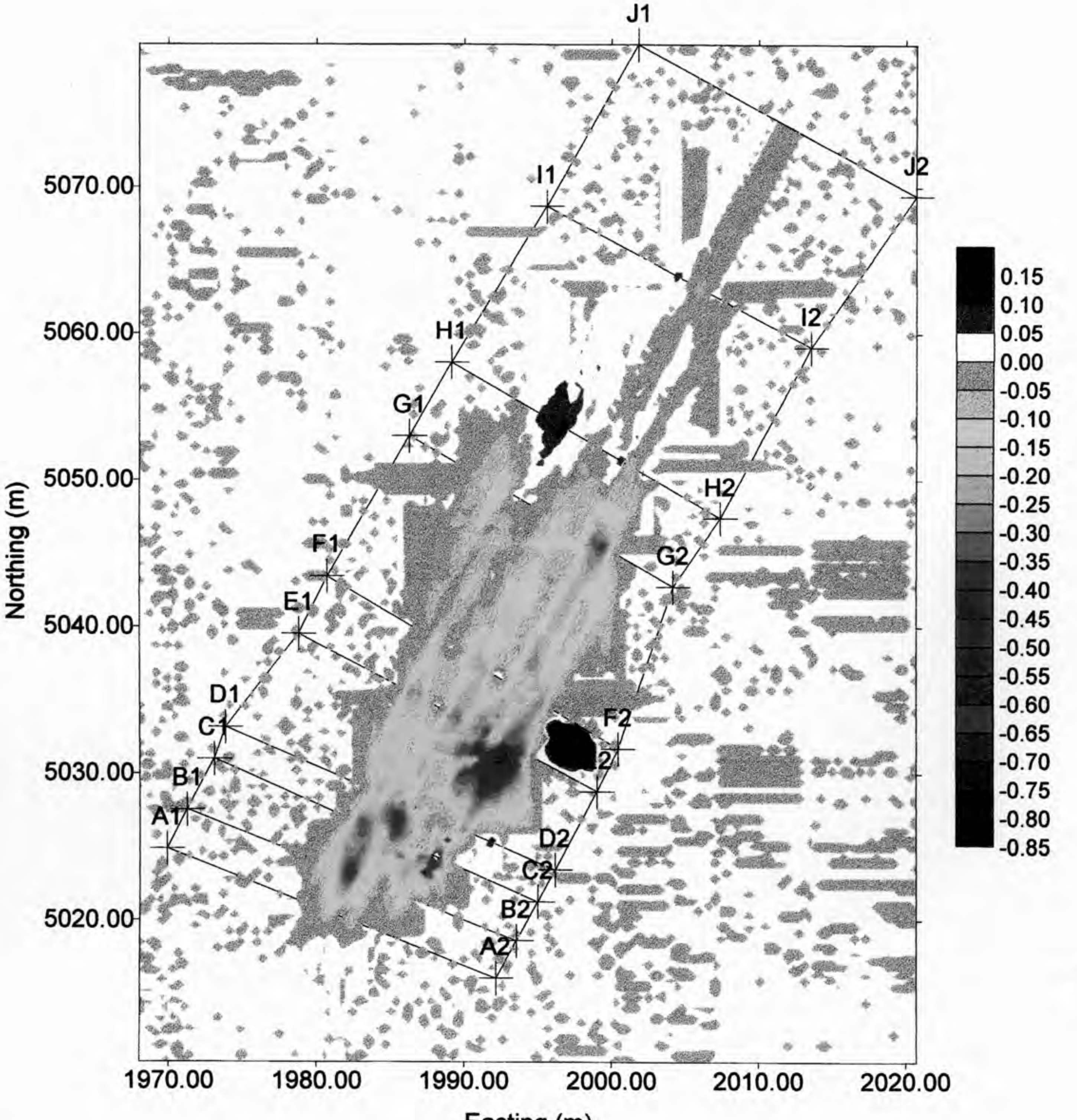

Figure 3.2.4: The results of the intensive cross-sectional analysis based on the 10 transects were translated to elevation data and used to evaluate the difference between measurements taken after each storm event. This figure illustrates the morphology of the batter slope from the initial surface to the storm event 261296, where erosion is represented on negative scale, whilst deposition is positive scale.

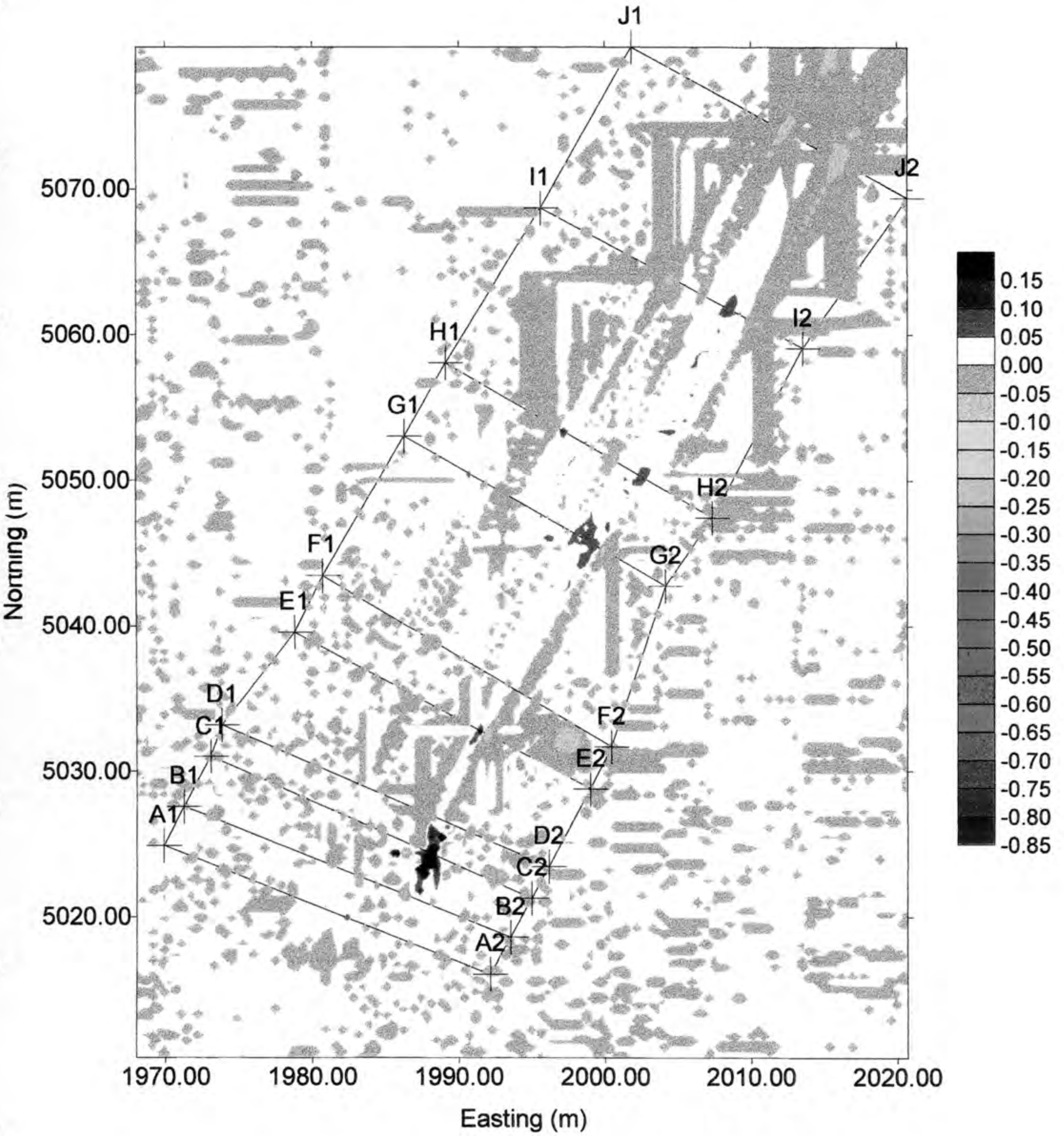

Figure 3.2.5: The difference between the surface profile at 261296, and 010197, where erosion is represented as positive values, and erosion as negative values. There was little alteration in the gully formation was associated with this storm event.

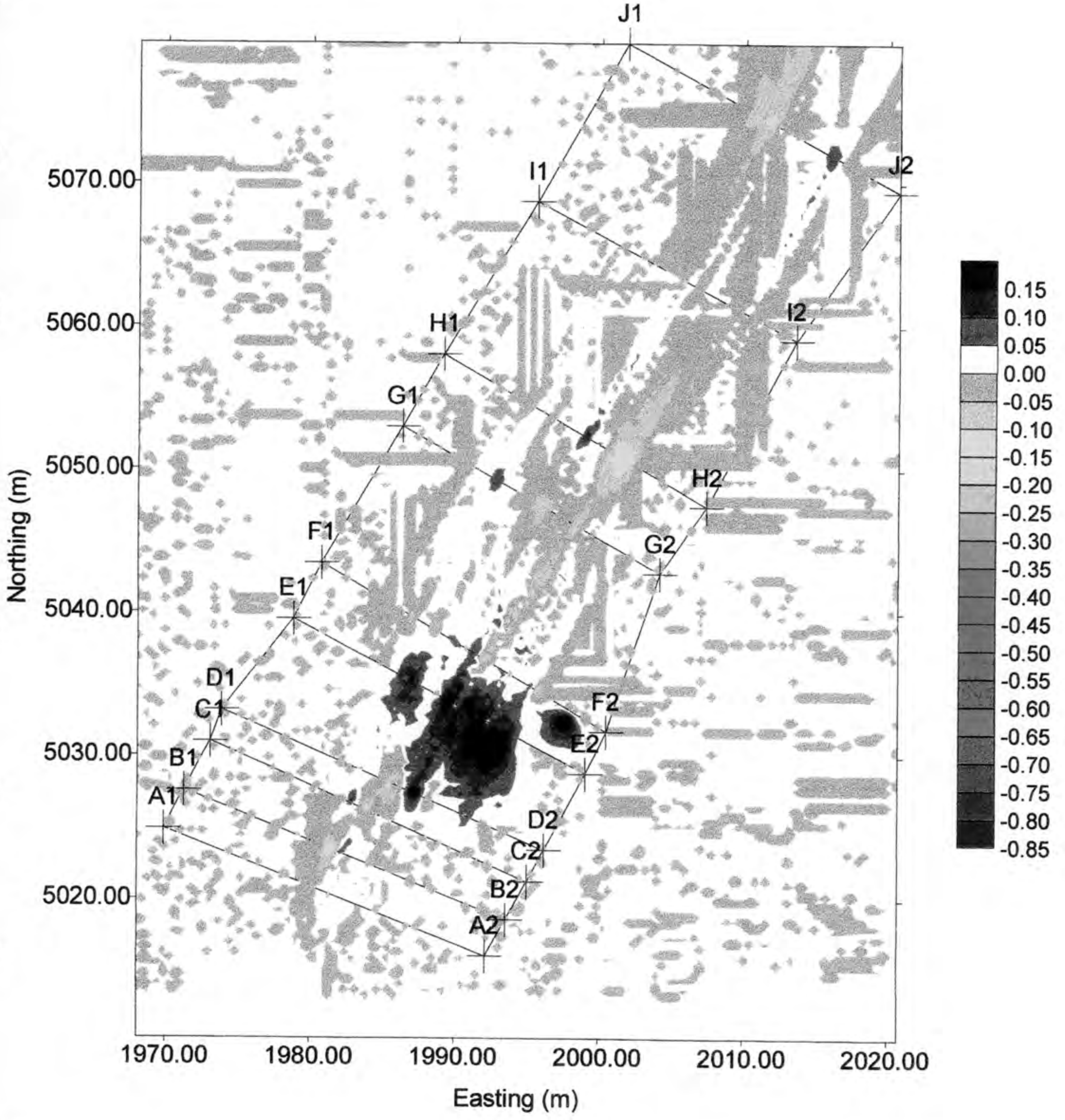

Figure 3.2.6: The difference between surface profile at 010197, and 230197. Erosion is once again represented on negative scale, whilst deposition is represented on positive scale.

Due to the large scale of mechanisms in operation, and as modelling discretisation consisted of a 20m by 60m grid (1m grid space) due to computational limitations, this was not considered beneficial.

Survey positions were taken at numerous random points in an attempt to enhance the findings from this aspect of the study, with a slightly better approximation being obtained in Figure 3.2.2, however it can be seen from the survey results conducted at the conclusion of the study that with approximately half the number of points recorded, a lot of detail was lost.

A physical description of the evolution of the gully helps to reaffirm those observations construed from the survey and cross-sectional analysis, with the characteristics of the formation of the gully remaining the most important aspects of the field study. Incorporation of other crucial sediment transport properties such as armouring can be identified readily in the upper sections of the gully after the initial event labelled 010197, with little movement occurring in these sections.

Figure 1.3.2 outlines the likely natural evolution of the steep batter slopes, with predictions based on work by Willgoose *et al*, 1992 suggesting that areas of deposition could be expected within 150 to 200m of the batter slopes, with depths of deposition up to 5m over the 1000 year time period.

From Figure 3.2.1, the initial excavation of the upper sections of the gully from Row A to Row C splits into two major arms, with accompanying deposition onto the divide between these arms, between sections Row D and Row E.

The actual initiation of the gully commenced a few days before the establishment of monitoring methods, with little data obtained and hydrological information about this storm event also being lost.

The first major event occurred on the 261296, with the event illustrated in Figure 3.2.7 occurring on the 191296. This event on 191296 was considered typical of the average storm events encountered during the monitoring period, with relatively even rainfall intensity and total rainfall level reaching 30 to 40mm.

However once the gully was instigated, erosion due to these relatively insignificant storm events was minimal. Although relatively little material was displaced by the preliminary event, the highly erodible upper surface material was quickly reduced about 10 to 20cm in some places. This was noteworthy due to the removal of almost all the finer material from the surface after the formation of the gully following the significant storm event occurring on 261296.

Figure 3.2.7 illustrates cross section located at the point now described as Row D. Although little material was mobilised from the upper surface of the batter slope, the earthworks in development of the catchment boundary wall and the channel linking the cap site to the remainder of the catchment, provided excess sediment during these initial events which was conveyed by the developing gully.

Figure 3.2.7 is compared with Figure 1.1.4, illustrating the batter slope before commencement of monitoring. The layout of the slope was relatively uniform, with little difference in elevation across the traverse. The inherent variability in the erodibility of the waste rock material is also indicated by this figure, material susceptible to geochemical weathering generated the material that was rapidly eroded once gully development commenced.

Other considerations included the nature of the pathway of the gully adopted, defined as the thalweg, minimal elevation point of the gully. This initial event dictated the shape of the formation of the gully during the remainder of the monitoring period. The consequent event, designated as the first major event excavated this cross-section dramatically, with little resemblance between the two surfaces.

Figure 3.2.9 illustrates the divide between each of the two major arms of the gully after the first major storm event, due to nature of inlet point, and armouring encountered within several centimetres of the upper surface.

The establishment of the reservoir above the entrance to the gully network contributed significantly to reducing the velocity of water in the upper sections of the gully. As the water reached the middle sections, the momentum had increased to such as extent that more significant amounts of material could be mobilised.

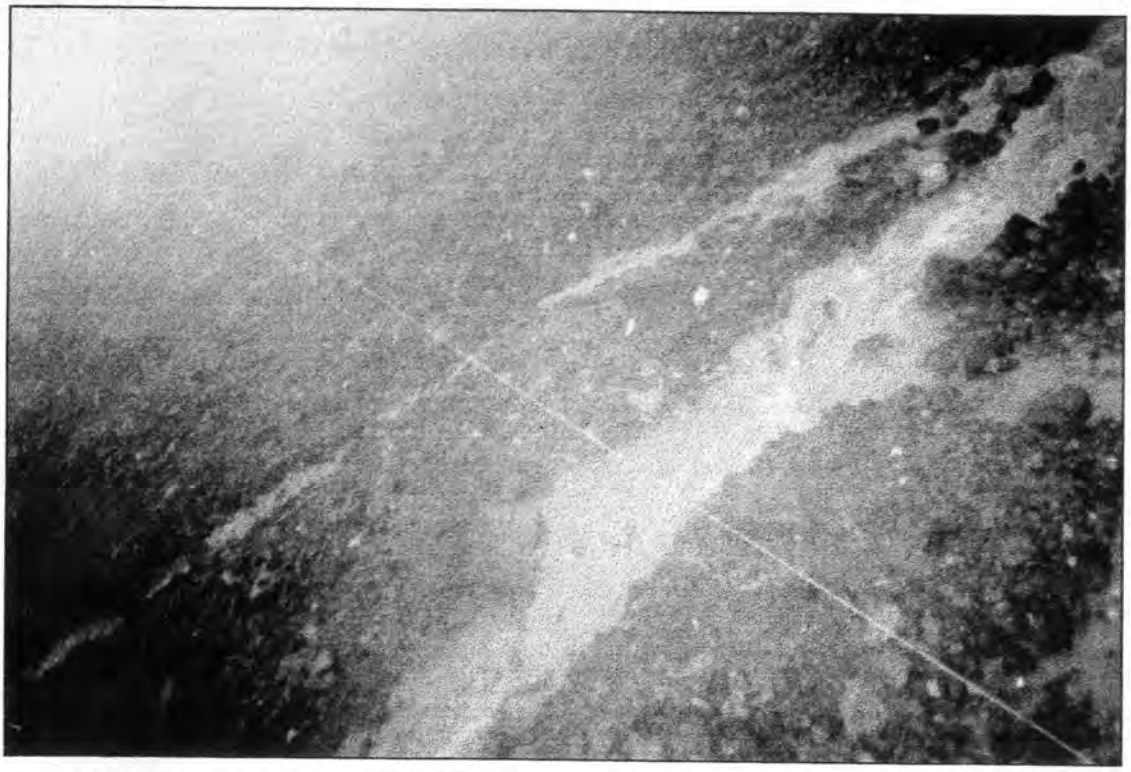

Figure 3.2.7: This cross-section was located at the point now labelled as Row D, with excavation of the loose upper surface material to some 10 to 20cm in depth. At this time little of the monitoring equipment had been established. It is also noted that this profile is not vertical, with the starpost in the upper left corner indicating the degree of elevation.

Figure 3.2.8: The first storm was estimated to be 30 to 40 mm, in total with incomplete installation of monitoring equipment resulting in no hydrological data obtained. However little emphasis was placed on this event, given the magnitude of the first significant event on 261296.

Although the constraint of the artificial reservoir may misrepresent what may happen considering the final design landform, the modelling process does not take into account the initial water velocity regardless, making this discrepancy less significant.

The nature of the waste rock material below the finer grade of material is evident in Figure 3.2.8 and Figure 3.2.9, with the relatively finer material seen centrally. The two arms of the gully were separated at the top of the batter slope due to the very large rock fragments encountered only several centimetres below the surface. The paths of the two arms crossed again below Row D with another tributary to the right of Figure 3.2.10.

Substantial deposition of 10 to 20cm in places at the forefront of the advancing major tributary continued until the end of this event. With large amounts of fine material deposited between Row G and Row H, which was consequently excavated in some degree by the more minor event on the 010197.

The gully extended to Row H during this event and is illustrated in Figure 3.2.11, and Figure 3.2.12, with the pathway becoming indistinct below Row I with deposited material (over erosion pin row 3) relatively easily erodible. It was noted that this event has a peak discharge of 21L/s, with rainfall continuing for approximately 1.5 hours, eroding the material transported initially.

The minor tributary on the right hand side of the slope encountered slightly less erodible material with mean particle diameter approximately twice that of the left hand side. The excavation of the gully halted about Row F to G for the major arm, and Row E to F for the minor arm. It was also noted that the paths of the two thalwegs crossed, and material deposited contributed to the overburden from the excavation of the sections above, as seen in Figure 3.2.11. This was also evident in Figure 3.2.5, with excavation divided between the two major arms, being clearly delineated. Overburden us highlighted in this figure, with minor disturbance of about 10 to 20cm being widespread between Row G and Row H.

Figure 3.2.9: The profile of the upper section was established by the first major storm event. Complete removal of fine material is evident in this figure and comparison is made to Figure 3.2.8 above.

Figure 3.2.10: The two main tributaries were separated between Row A to Row D, with thalwegs crossing below Row D as pictured here. Another tributary developed to the right of this photo, which crossed again below Row E to Row F in consequent events.

Figure 3.2.11: The removal of fine material was more widespread below Row D, as seen by the painted fluorescent lines across the slope. Both channels combined, and the gully pathway was not easily discernible.

Figure 3.2.12: The left tributary also continued down the hillslope with relatively easily erodible material deposited between Row H and Row I making the pathway adopted distinct in the background of this photo.

The diversion of flow into the major gully from the divide pictured in the upper sections of the slope, resulted in significantly more erosion on this side, below Section F2 to Section G2. About one third of the flow was diverted to this path, with this gully ceasing to advance once past the intersection between the concave and convex parts of the batter slope, the point of change in curvature.

The next rainfall event occurred in 010197 with total rainfall of 60mm, and peak discharge entering the gully at 13 L/s, with average 4 L/s. This storm was monitored with a photographic record available. The amount of material moved by this event was considerably less due to the reduced intensity, as well as extensive armouring exhibited in the upper regions from initial activity.

Although the catchment had been constructed for same time, since the first event on 191296, the remnant brown mud sediment is evident in the suspended flow entering the gully in Figure 3.2.12. The buffering effect of the gully is also evident in this figure with flow diverging into the two main arteries. The accumulation of water behind the leading edge of bund wall supplied water to the gully for several hours after the rain had ceased, effectively minimising initial discharge velocity.

The divide between the two main tributaries is still evident in Figure 3.2.13, with coalescing of gully pathways below Row D to Row E pictured in Figure 3.2.14. The fluorescent paint used to delineate the previously eroded sections and was particularly useful in outlining the pathway of the gully as it developed.

The survey results pictured in Figure 3.2.2, were used to derive a directional derivative approximation of the drainage network for the gully, and this appears in Figure 3.2.15.

The third and final significant storm event occurred on 230197, with total rainfall of 45mm, over a period of only 30 mins, with peak discharge 29L/s.

Although Figures 3.2.4, Figure 3.2.5, and Figure 3.2.6 represent a morphology of the landform over a small duration, the inherent lack of detail devised from the cross-sectional analysis allows only generalisations to be made. Extrapolation of the cross-section of the gully at the transects located at both Row F and Row G by the mapping

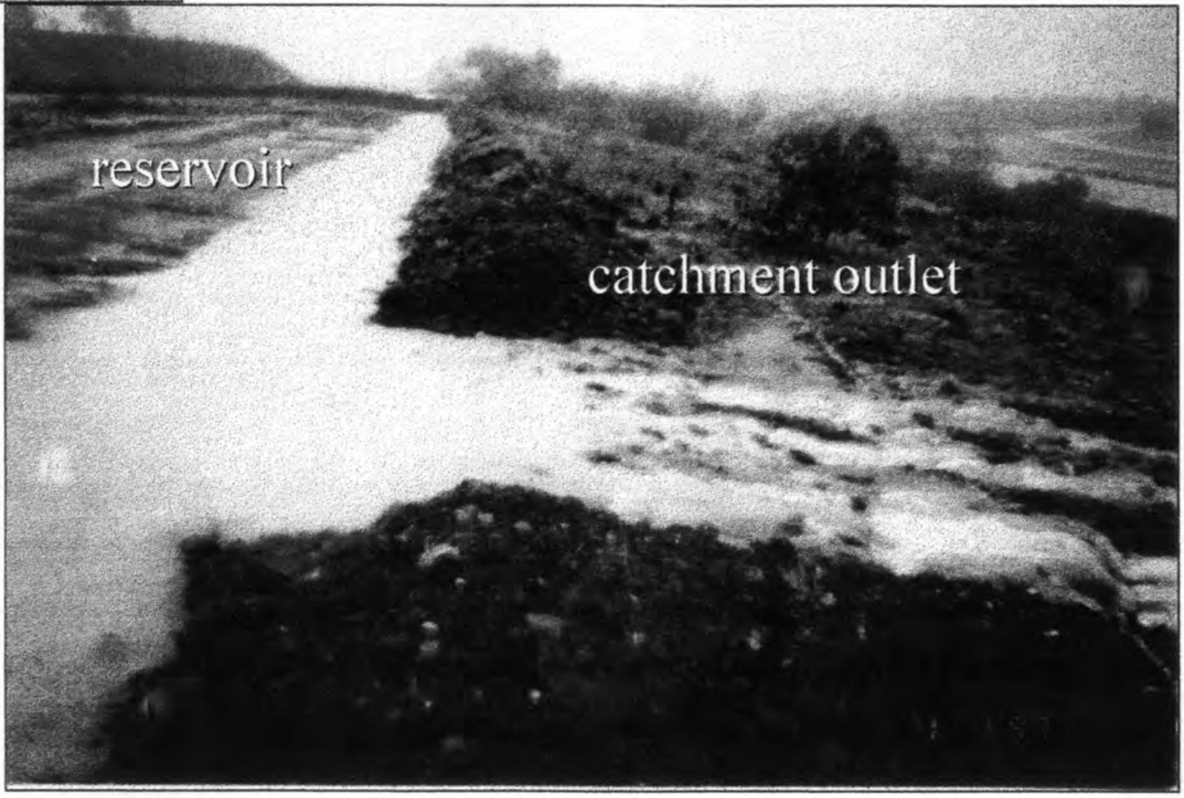

Figure 3.2.13. The inlet point of the catchment extended ~ 3m with approximates of 2m and 4m used during the modelling process.

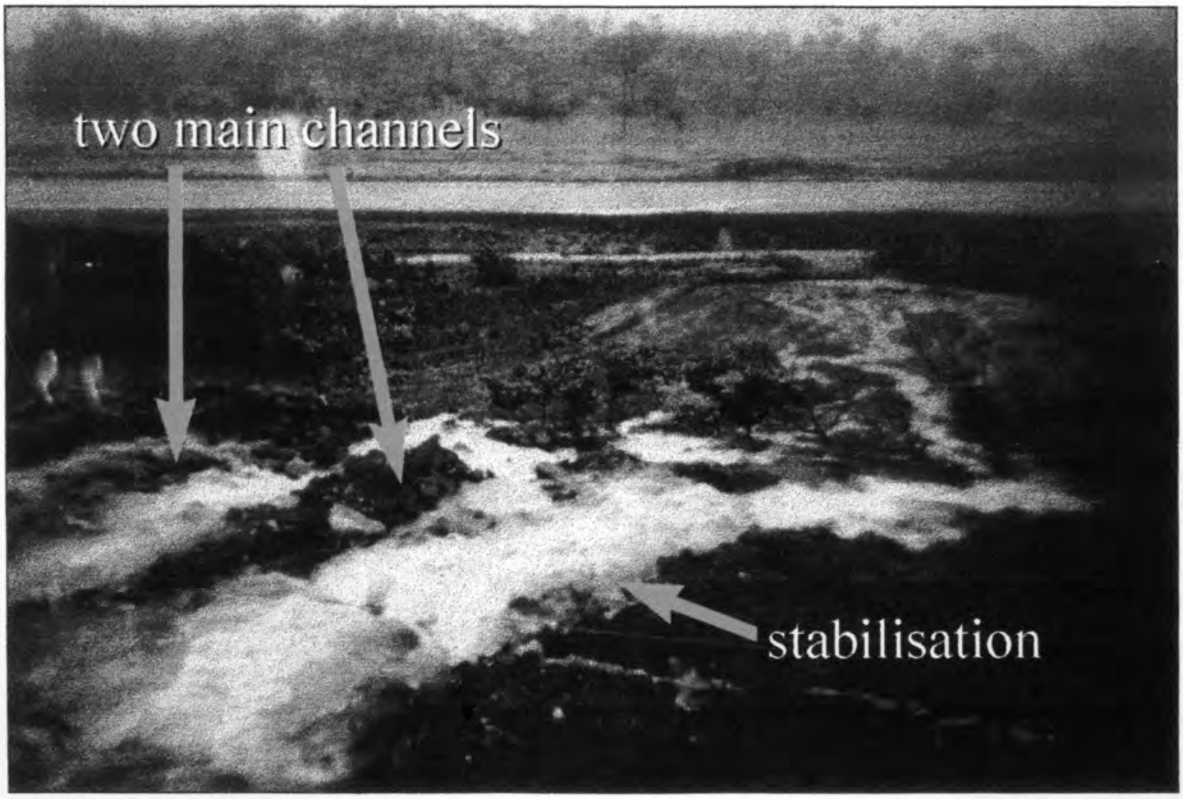

Figure 3.2.14. The pathway of the gully can be delineated by the fluorescent paint markings, indicating regions that were eroded on deposited between each storm event.

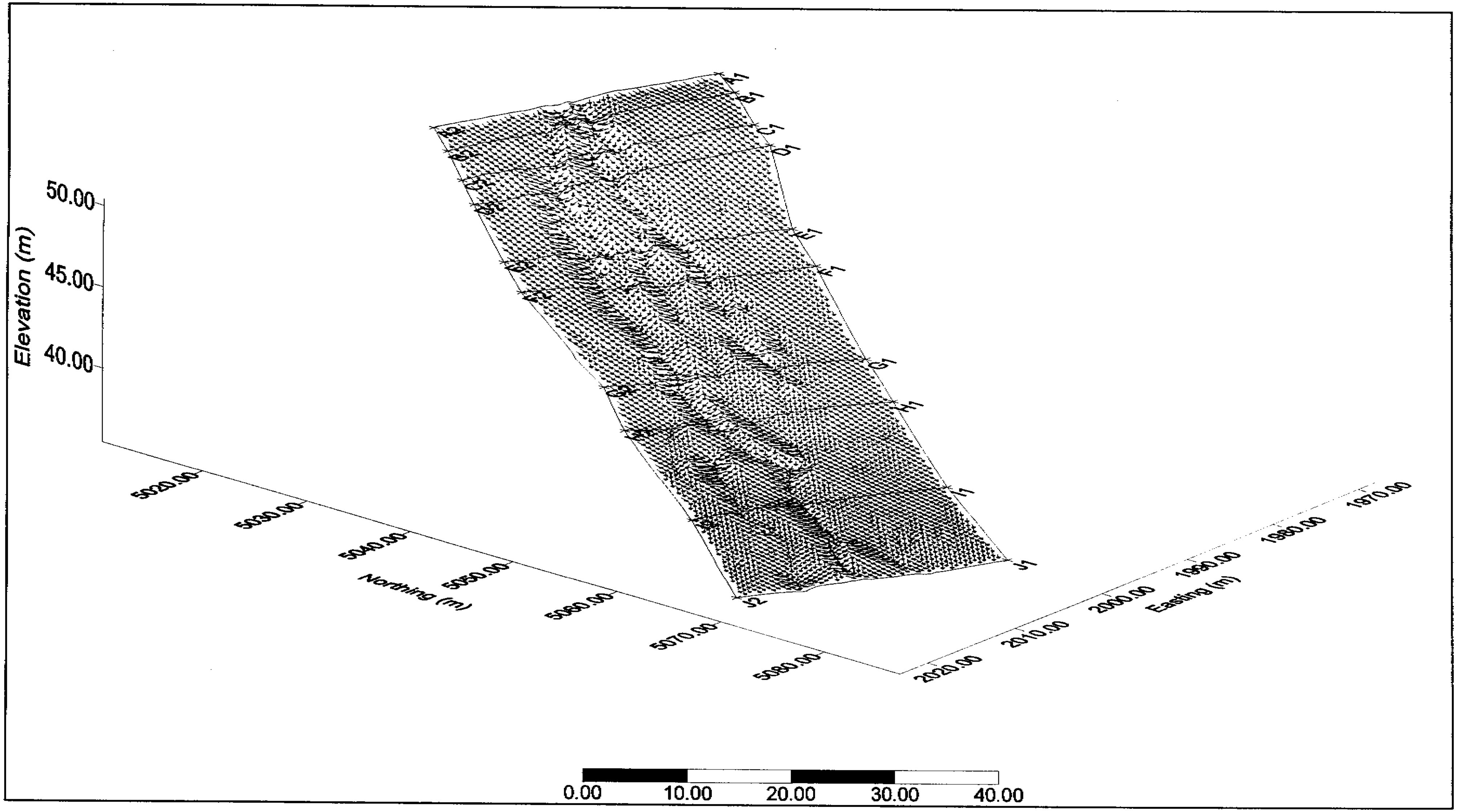

Figure 3.2.15: The survey conducted mid-way through the monitoring period was used to generate a directional derivative schematic of the drainage pattern for the gully.

Table 3.2.1: The amount of material excavated or deposited by each event was approximated by the subtraction of the upper surface from the lower surface. Estimates of net deposition can be seen in the events at the end of the monitoring period.

Description	*Erosion Volume (m^3)*	*Deposition Volume (m^3)*	*Morphology (m^3)*
Transect-261296	52.29	5.55	46.74
Transect-010197	5.25	6.94	-1.68
Transect-230197	8.42	13.93	-5.51
Survey-160197	68.90	30.14	38.76

Table 3.2.2: The width of the gully as it developed, is noted not to change significantly due to the extensive armouring experienced at the top of the batter slope, and the low initial velocity due to the artificial reservoir.

ROW: dated 28/12/96.	*Width (m)*	*Location (m..m).*
R1-R2 (2.9m)		**Using R1**
At 1m from R1	**2.05m**	**10.55m to 12.60m**
	1.60m	**13.20m to 14.80m**
At 2m from R1	**1.95m**	**10.60m to 12.55m**
	1.95m	**13.15m to 15.10m**
R2-R3(3.4m)		**Using R2**
At 1m from R2	**0.55m**	**10.00m to 10.55m**
	2.37m	**11.35m to 13.72m**
	1.30m	**15.20m to 17.00m**
At 2m from R2	**0.35m**	**10.00m to 10.35m**
	2.40m	**10.90m to 12.30m**
	1.00m	**12.70m to 13.70m**
	1.80m	**15.20m to 17.00m**
R3-R4(2.6m)		**Using R3**
At 1m from R3	**4.45m**	**10.55m to 15.00m**
	1.70m	**16.10m to 17.80m**
R4-EP1 (3m)		**Using R4**
At 1.5m from R4	**1.15m**	**11.65m to 12.80m**
	1.55m	**13.70m to 15.25m**
	1.75m	**15.65m to 17.40m**
	2.70m	**18.00m to 20.70m**
EP1-R5 (3.6m)		**Using R5**
At 2m from EP1	**1.85m**	**8.75m to 10.60m**
	1.80m	**11.20m to 12.00m**
	3.40m	**13.30m to 16.70m**
R5-R6 (3.6m)		**Using R5**
At 2m from R5	**1.10m**	**8.00m to 9.10m**
	1.30m	**11.70m to 13.00m**
	1.70m	**13.30m to 15.00m**
	2.20m	**15.40m to 17.60m**
R6-EP2 (7.9m)		**Using R6**
At 3m from R6	**1.40m**	**6.60m to 8.00m**
	1.70m	**8.30m to 9.00m**
	1.90m	**10.20m to 12.10m**
At 6m from R6	**0.75m**	**6.80m to 7.55m**
	1.75m	**8.45m to 10.30m**
	2.20m	**10.80m to 13.00m**
	3.20m	**14.10m to 17.30m**
EP2-R7 (3.8m)		**Using R7**
At 2m from EP2	**1.10m**	**5.00m to 6.10m**
	1.45m	**7.20m to 8.65m**
	1.10m	**14.10m to 15.20m**
R7-R8(5.7m)		**Using R7**
At 3m from R7		**7.35m to 8.50m**
		11.60m to 13.00m
		14.00m to 16.00m
R8-EP3 (5.2m)		**Using R8**
At 3m	**1.00m**	**7.50m to 8.50m**
	1.70m	**9.20m to 10.90m**
	3.60m	**11.70m to 14.30m**
EP3-R9 (7.8m)		**no**
R9-EP4 (6.9m)		**significant**
EP4-R10 (5.7m)		**formations**
R10-EP5 (9.2m)		**here as yet.**

package tended to conceal the complex nature of activity in those sections. From Figure 3.2.4, the areas of deposition are less clear, however with comparison with the results presented in Figure 3.2.2 the sections from Row F to Row G allows insight into the nature of this mechanism.

The disturbed sections of the batter slope were cleared of fine particles, resulting in dramatically reduced erodibility. From Figure 3.2.8, the disturbed material could be used to easily identify the path of the minor tributary, with erosion pins dislodged and transported downstream below transect Row D. Below the trees in the middle ground of the photo, a pathway linking the two major arms of the gully crosses. Overburden from this intersection deposited during the end of the initial event, as well as that of the 010197 storm event, with significant scouring observed during the final event.

The layering of fine mulch is of concern in future investigations, with depth in Row G to H about 50 to 60cm, revealed by examination of sidewall of the main gully. The relative heterogenous nature of fine particles is observed in photographic series in Figure 3.2.16 to Figure 3.2.19, where a 30cm ruler is highlighted in the centre of most of these figures.

Some sections of the gully, once breached eroded quickly with soft earthen material excavated from just above the mined ore, being exposed in Figure 3.2.8. A combination of surface layers has been used to design the batter slope, (pers com. Willgoose, 1997) making excavation to this depth, of some concern.

Further evaluation of the role of rapid geochemical weathering, and impact of diffusive mechanisms on modelling simulations may need to be conducted.

Figure 3.2.16: Excavation of sidewall material slowly increased the width of the gully, with residual layer of fine material about 45cm accumulating at this point.

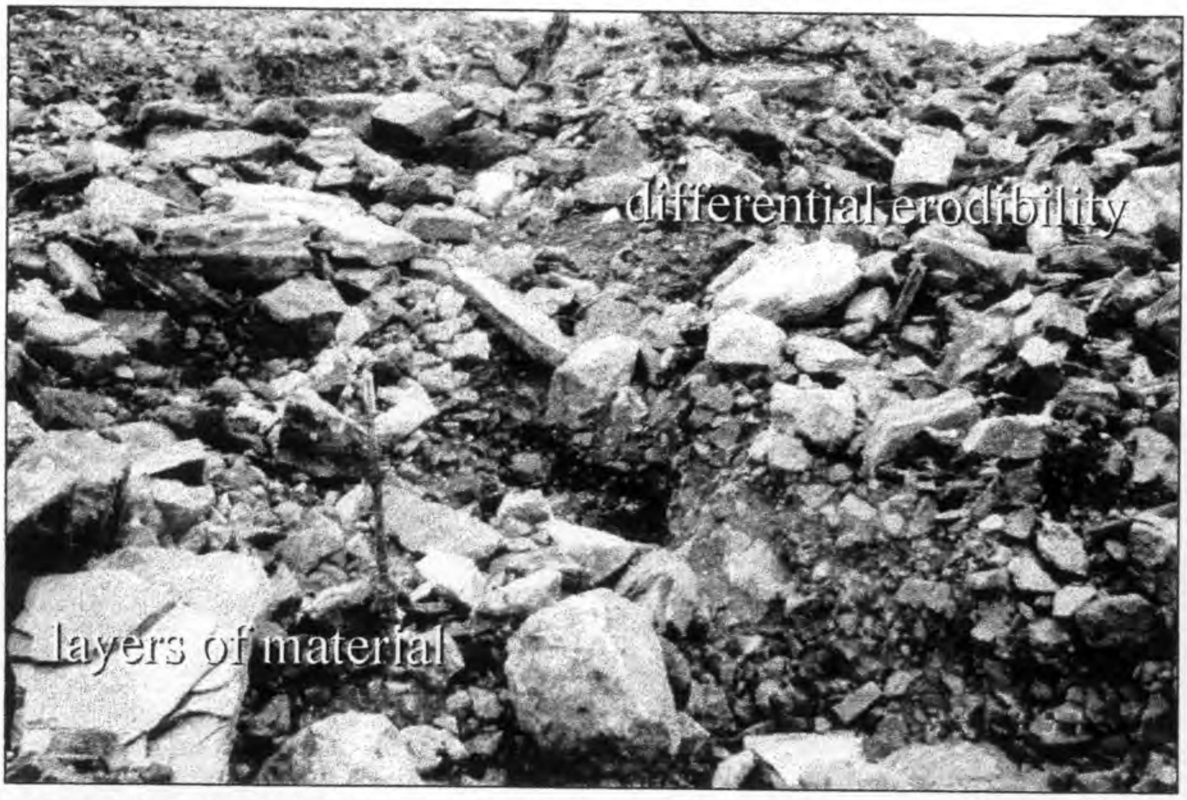

Figure 3.2.17: The depth of erosion reached 60cm in some places, revealing the heavily armoured rock fragment layer. The differential erodibility of these surfaces is considered with the soft earthen material extracted from above the mined ore seen as brown colour. Depth-erodibility relationships for this slope would therefore be complex, once the protective layer is breached.

Figure 3.2.18: The excavation of material from Row H to Row I, reaches a depth of 60cm with large rock fragments armouring further incised.

Figure 3.2.19: The gully extends to Row I with depth of 20cm to 30cm, whilst almost reaching the concrete apron of the flume pictured in background.